International Journal of Scientific & Engineering Research, Volume 4, Issue 8, August 2013
ISSN 2229-5518

Synthesis and study of $Ce_xPr_xMg_{1-2x}Al_2O_4$ ceramic pigment by combustion method using malonic acid dihydrazide as fuel

Ayman Awad Ali, Bekir Karasu, Mahmud Rustam Allazov, Teymur Mamed Ilyasli

Abstract—Nanoparticle $Ce_xPr_xMg_{1-2x}Al_2O_4$ system ceramic pigments were prepared from the mixture of aluminum, magnesium, cerium and praseodymium nitrates ignited with malonic acid dihydrazide as a fuel following by annealing at different calcinations temperatures. The chemical structure, phase formation and spectral characterization of pigments are characterized by different tools such as thermal analysis (TG-DTA), x-ray diffractions (XRD), transmission electron microscopy (TEM) and infrared spectroscopy (IR). The colors of inorganic pigments are determined by diffuse reflectance spectroscopy (DRS) using CIE-L*a*b* parameters method for color measurements.

Keyword: x-ray diffractions; nanomaterials; ceramic pigment

1 INTRODUCTION

Combustion synthesis or fire synthesis is also known as self-propagating high temperature synthesis and highly exothermic redox chemical reactions between an oxidizer and a fuel as urea, carbohydrazide, glycine, oxalic acid dihydrazide, alanine, malonic acid dihydrazide, sucrose [1-2] and other. The oxidizer/fuel molar ratio (O/F) =1 is considered the perfect ratio for combustion synthesis which produce amount of energy sufficient to prepare the corresponding oxides [3]. We were used combustion synthesis because of safe, simple, rapid fabrication process, and saves both time and energy. It can be used to prepare highly pure, homogeneous and crystalline with nano-particle sizes [4-5]. Magnesium aluminate spinel is an important functional ceramic materials, because of its high melting point (≈2135°C), good mechanical strength and high resistance to chemical attack, excellent optical and dielectric properties. It has been applied in various applications, such as in the cement and steel industry [6-7], transparent windows and lenses for the infrared and visible regions [8], military applications, humidity sensors [9–11], catalysts [12] and other. We were synthesized $MgAl_2O_4$ spinel doped with cerium and praseodymium oxides as solid solution for importance as red orange ceramic pigment agent.

2 EXPERIMENTAL

2.1 MATERIALS

The starting chemicals used in this study are aluminum nitrates pentahydrate, $Al(NO_3)_3 \cdot 9H_2O$ (Aldrich), magnesium nitrates hexahydrate, $Mg(NO_3)_2 \cdot 6H_2O$ (Aldrich), praseodymium oxides Pr_2O_3 (Aldrich), cerium carbonates $Ce_2(CO_3)_3$ (Aldrich), nitric acid 65%, diethyl malonate 99.9% (Aldrich) and hydrazine hydrate (Aldrich).

2.2 SYNTHESIS

2.2.1 Synthesis of malonic acid dihydrazide (MDH), $C_3H_8N_4O_2$

Malonic acid dihydrazide (MDH) was prepared by the chemical reaction of 1 mol of diethyl malonate with 2 mol of hydrazine hydrate [1,3]. The chemical reaction is written as follows eq. 1:

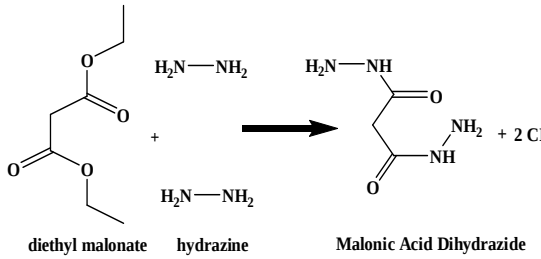

(1)

2.2.2 Synthesis of ceramic pigment

$MgAl_2O_4$ spinel powders doped with praseodymium and cerium oxides were prepared by combustion synthesis using malonic acid dihydrazide as fuel. Praseodymium oxides and cerium carbonate dissolved in small amount of nitric acid at hotplate (60-70 for 5 min.). The calculated stoichiometric amounts of metal salts (aluminum nitrates, magnesium, cerium and praseodymium nitrates) were dissolved in distilled water and mixed with malonic acid dihydrazide according to equation 2. The resulting precursor was transferred into furnace that preheated to 250-300°C, evaporated and spontaneously ignited exothermic reaction by ignition of the metal nitrates and organic material with the release of gases. The combustion reaction completed within a few seconds, producing a precursor of oxides which was annealed at 800, 1000 and 1200°C for 2h.

- *Ayman Awad Ali Currently Pursuing Ph.D Degree in chemistry, Benha University, Faculty of Science, Chemistry Department, Benha, Egypt, , e-mail: pigment23@gamil.com*
- *Bekir Karasu, Anadolu University, Engineering Faculty, Materials Science and Engineering Department, Eskisehir,Turkey, e-mail: bkarasu@anadolu.edu.tr*
- *Mahmud Rustam Allazov, Baku State University, Chemistry Faculty, Inorganic Department, Baku, Azerbaijan, e-mail: allazov_m@mail.ru*
- *Teymur Mamed Ilyasli, Baku State University, Chemistry Faculty, Inorganic Department, Baku, Azerbaijan, e-mail: teymur.ilyasly@mail.ru*

International Journal of Scientific & Engineering Research, Volume 4, Issue 8, August 2013
ISSN 2229-5518

$$2(1-2x)\ Mg(NO_3)_2.6H_2O + 4Al(NO_3)_3.9H_2O + 2xPr(NO_3)_3.6H_2O + 2xCe(NO_3)_3.6H_2O + (5+5x/4)\ C_3H_8N_4O_2 \longrightarrow 2Ce_xPr_xMg_{1-x}Al_2O_4 + 68H_2O + (15+15x/4)CO_2 + (18+11x/2)N_2 \quad (2)$$

2.3 characterization

Thermal analysis (TGA; Simultaneous TG-DTA/DSC Apparatus "STA 449 F3 Jupiter") of the precursor carried out at a heating rate of 10°C/min in static air. Phase formation of product identified by using X-ray diffraction (XRD; advanced D8) with Cu Kα radiation and the wavelength equal to (0.15406 nm). Transmission electron microscopy (TEM, modal: Tecnai G20, super twin, double tilte, at 200 kV and magnification up to 1000000 x). Infrared (IR) samples were carried out by using Jasco FT/IR-460 plus spectroscopy in 400–4000 range by employing potassium bromide KBr, pellet technique. The diffuse reflectance of fired pigments measured in Jasco spectrophotometer UV–Vis in 300–800 nm range using standard D65 illumination and barium sulfate as a reference. The CIE L*a*b* colorimetric method, recommended by the Commission Internationale de l'Eclairage (CIE) [13] followed. In this method, L* is lightness axis: black (0) – white (100), b* is the blue (−) – yellow (+), a* is the green (−) – red (+) axis and E is the hue variation, $\Delta E^2 = (L^*)^2 + (a^*)^2 + (b^*)^2$ and the parameter C* (chroma) represents saturation of the color and h^o represents the hue angle. The parameter C* (chroma) represents saturation of the color and h^o represents the hue angle. The chroma is defined as $C^*=[(a^*)^2+(b^*)^2]^{1/2}$. The hue angle, h^o is expressed in degrees and ranges from 0^o to 360^o and is calculated using the formula $h^o = \tan^{-1}(b^*/a^*)$.

3 Result and Discussion

3.1 Thermal analysis

TG/DTA curves of $Ce_{0.1}Pr_{0.1}Mg_{0.8}Al_2O_4$ ash shown in figure 1. TG curve of $Ce_{0.1}Pr_{0.1}Mg_{0.8}Al_2O_4$ show three steps. In TG curve for $Ce_{0.1}Pr_{0.1}Mg_{0.8}Al_2O_4$, the first step occurred in range 80-300°C with weight loss equals to 7 %, the second step in range 300-600°C losses 7% and the third step in the range 600-850°C losses 11 %. The first step for two sample were occurred for elimination of the humidity and co-ordination water and the second and the third due to evolution of CO, CO_2 and NOx gases from sample as result of the decomposition the residual of organic material. From TG curve, we can say that phase formation starts around 800°C for $Ce_{0.1}Pr_{0.1}Mg_{0.8}Al_2O_4$ comparison with $MgAl_2O_4$ which formed by the same fuel and the phase formation starts around 750°C [14]. DTG curve of $Ce_{0.1}Pr_{0.1}Mg_{0.8}Al_2O_4$ shows three endothermic peaks at 100, 400 and 660°C. DTA curves of $Ce_{0.1}Pr_{0.1}Mg_{0.8}Al_2O_4$ shows two endothermic steps at 100 and 825 °C and two exothermic steps at 330°C and 450°C. The first endothermic step occurred for elimination of the water in sample. The exothermic steps occurred for elimination and oxidation of the residual organic material in sample. The third endothermic reaction step shows phase formation and appearance of phase under study [15]. We can say that the phase formation starts at 825°C for $Ce_{0.1}Pr_{0.1}Mg_{0.8}Al_2O_4$

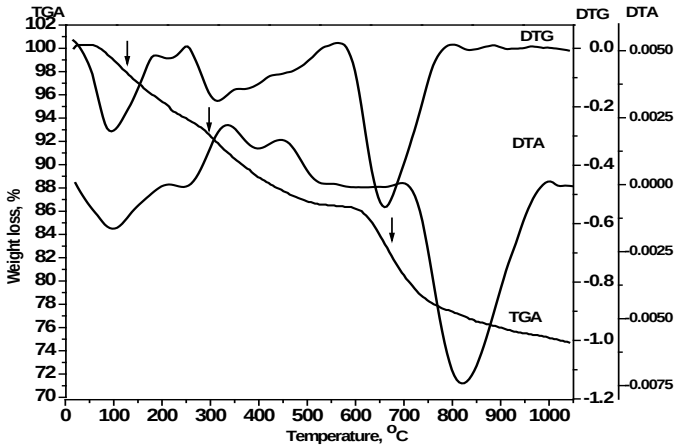

Fig 1. Thermal analysis (TG, DTG and DTA) of ash for a) $MgAl_2O_4$, b) $Ce_{0.1}Pr_{0.1}Mg_{0.8}Al_2O_4$

3.2 Infrared Spectra (FTIR)

The IR of $Ce_{0.1}Pr_{0.1}Mg_{0.8}Al_2O_4$ system (where x=0.00, 0.05 and 0.1) are studied at different calcinations temperatures and noted in table 1. In the 800–4000 cm-1 region of the IR spectrum, the absorption bands at 3614-3400 cm-1 and 1647-1636 cm-1 for different systems at 300 and 1000°C/2h can be attributed to the presence of absorbed water or surface hydroxyl groups and free or crystal water. The intensity of the peak at 2928-1428-1385-800 cm-1 may be derived from the vibration of CH, NO_3 or NOx which decreases gradually as increased annealing temperatures. In the 800–400 cm^{-1} region of the IR spectrum, the weakness of the two bands at 300°C that they are low crystalline. The bands noted in table 1 are corresponding to the lattice vibration of AlO_6 and MgO_4 groups at 1000°C for different systems [14,16] which indicate to the formation of $MgAl_2O_4$ spinel.

Table 1. The assignment of the important functional groups in FTIR spectra for different system

T	Systems and phase	Functional groups, cm^{-1}			
		-OH	O-H	N=O	M-O
300	$MgAl_2O_4$	3456	1636	1385-800	683-451
	$Ce_{0.05}Pr_{0.05}Mg_{0,90}Al_2O_4$	3614	1647	1404-800	687-490-417
	$Ce_{0.1}Pr_{0.1}Mg_{0,8}Al_2O_4$	3400	1639	1400	700-586-421
	CeO_2	3429	1639	1400	650-529-430
1000	$MgAl_2O_4$	3449	1639	1400	698-513
	$Ce_{0.05}Pr_{0.05}Mg_{0,90}Al_2O_4$	3425	1639	1400	702-560-494
	$Ce_{0.1}Pr_{0.1}Mg_{0,8}Al_2O_4$	3437	1639	1400	706-517-459
	CeO_2	-	-	-	650-500-420

3.3 X-ray diffraction

The X-ray diffractions for $Ce_xPr_xMg_{1-2x}Al_2O_4$ system (where x= 0.00, 0.05 and 0.1) are studied at different annealing temperatures as shown in Figure 2. The peaks intensities of x-ray mean that crystallites of samples start after annealing at 800°C. It agrees will with data of thermal analysis for the formation of the stable spinel phase around 800°C. The intensities of peaks increase gradually with annealing until sharpen peaks are observed at 1000 and 1200° C. Figure 4 shows the relation between the particle sizes of sample at different calcinations temperatures [8,10,14]. The average

International Journal of Scientific & Engineering Research, Volume 4, Issue 8, August 2013
ISSN 2229-5518

crystallite size was calculated based on the XRD patterns using the peaks corresponding to the (h k l) planes and the scherrer equation 3:

$$\mathbf{D_{XRD} = (0.9\lambda)/(\beta \cos\theta)} \qquad \mathbf{3}$$

Where DXRD is the crystallite size (nm), λ is the radiation wavelength (0.15406 nm), β is the full width at half of the maximum (radians), θ is the Bragg angle (degrees). The crystalline particles size increase with increasing annealing temperatures. The particles sizes, densities, lattice parameter of different annealing temperatures from XRD data are given in Table 1.

Table 2. The particles sizes, densities, lattice parameter from XRD data

T,°C	system	D_{av}, nm	phase	color
800	$MgAl_2O_4$	10	S	white
	$Ce_{0.05}Pr_{0.05}Mg_{0.9}Al_2O_4$	8.9	S+ C	Orange
	$Ce_{0.1}Pr_{0.1}Mg_{0.8}Al_2O_4$	6.6	S+ C	orange
	CeO_2	31	C	yellow
1000	$MgAl_2O_4$	10.5	S	white
	$Ce_{0.05}Pr_{0.05}Mg_{0.9}Al_2O_4$	9.4	S+ C	orange
	$Ce_{0.1}Pr_{0.1}Mg_{0.8}Al_2O_4$	10	S+ C	orange
	CeO_2	32	C	yellow
1200	$MgAl_2O_4$	12.5	S	white
	$Ce_{0.05}Pr_{0.05}Mg_{0.9}Al_2O_4$	10.2	S+ C	orange
	$Ce_{0.1}Pr_{0.1}Mg_{0.8}Al_2O_4$	13.13	S+ C	orange
	CeO_2	33	C	yellow

S means $MgAl_2O_4$ spinel and C means CeO_2

3.4 Transmission Electron Microscopy, TEM

Figure 3 shows the TEM micrograph of the $Ce_{0.1}P_{0.1}Mg_{0.8}Al_2O_4$ and $MgAl_2O_4$ samples annealed at 1000 °C with sheet and spherical shapes. The distribution of particle sizes for $Ce_{0.1}P_{0.1}Mg_{0.8}Al_2O_4$ and $MgAl_2O_4$ are 7-14 nm and 8–15 nm in TEM micrograph, respectively. A mean average particle size calculated by averaging approximately thirty particles measurement is about 11 nm for $MgAl_2O_4$ and 12 nm for $Ce_{0.1}P_{0.1}Mg_{0.8}Al_2O_4$. The particle sizes are determined using TEM and are compared with that obtained from XRD and collective data. These sizes agree with XRD data, indicating that the particles observed by TEM are primary particles [8, 10].

3.5 Reflectance spectra

The diffuse reflectance spectra of pigments powder at different annealing temperature shown in figure 4. Pigments are insoluble in concentrated acid or base and did not affect the intensity of color. The study of doping of spinel structure MgAl2O4 with Ce and Pr oxide to producing colored ceramic materials, CePr:$MgAl_2O_4$ ($MgAl_2O_4$ and $CePrO_{2-\delta}$). The light yellow color of CeO_2 only or inside $MgAl_2O_4$ as result of the charge transfer transition between O2p and Ce4f conduction band of Ce^{4+} (band gap=2.76). The doping this system (Ce:MgAl2O4) with Pr^{4+} ($4f^1$) introduce an additional electron to electron to charge transfer transition between O_{2p} and Ce_{4f} and reduce the band gap from 2.76 to 1.7 eV. The present of Pr^{4+} shifted the color from yellow to red color. We studied the color of these compounds at different temperatures and color parameters summarized in table 3.

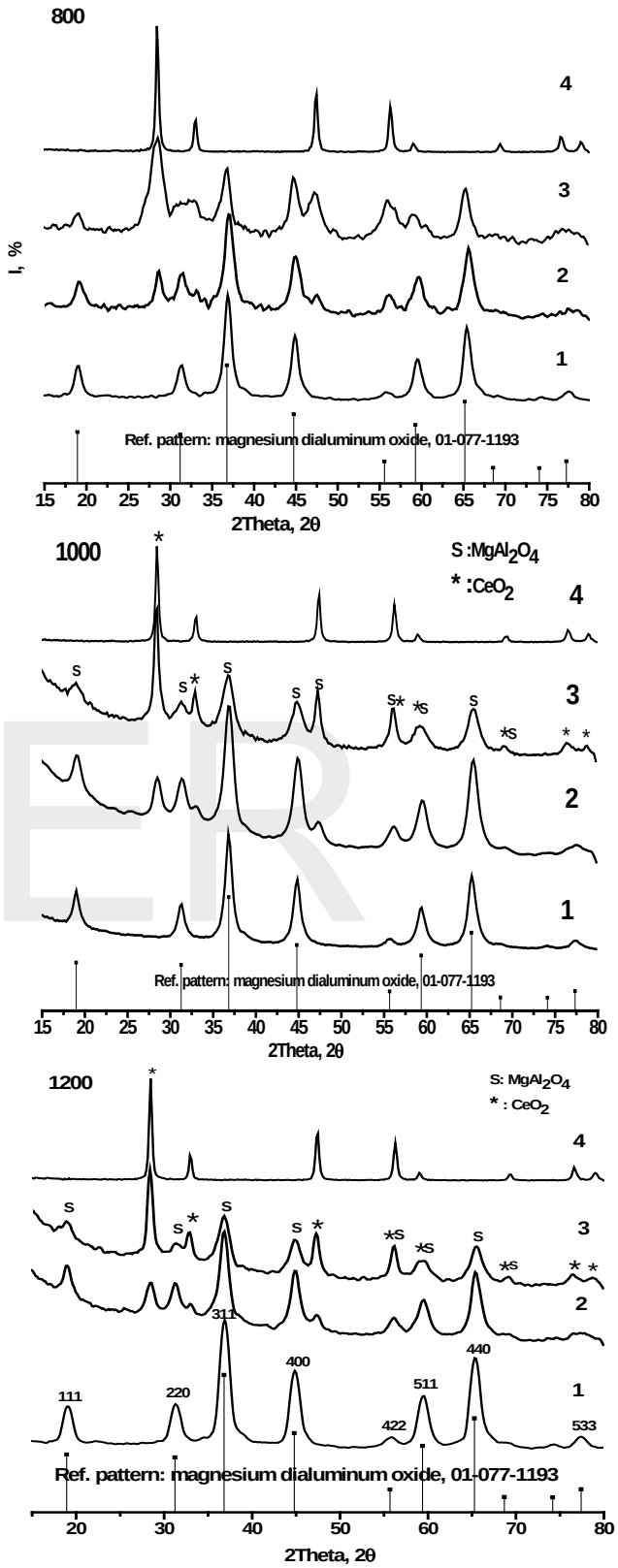

Fig.2. X-ray diffraction for 1) $MgAl_2O_4$, 2) $Ce_{0.05}Pr_{0.05}Mg_{0.90}Al_2O_4$, 3) $Ce_{0.1}Pr_{0.1}Mg_{0.80}Al_2O_4$ and 4) CeO_2 at 800, 1000 and 1200°C.

International Journal of Scientific & Engineering Research, Volume 4, Issue 8, August 2013
ISSN 2229-5518

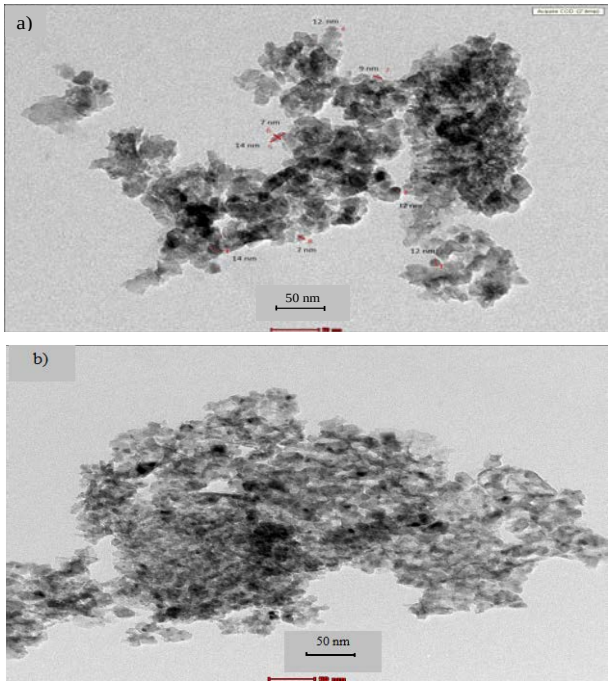

Fig 3(a and b). Transmission electron microscopy for a)$MgAl_2O_4$, b)$Ce_{0.1}P_{0.1}Mg_{0.8}Al_2O_4$ annealed at 1000°C.

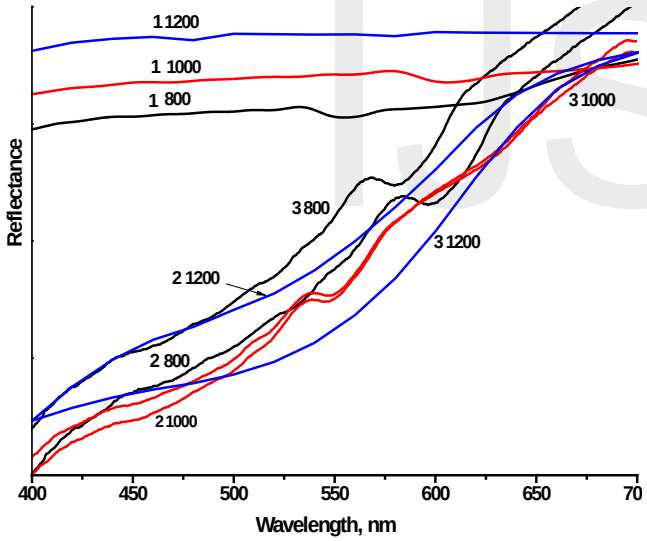

Fig 3. Reflectance spectra of 1)$MgAl_2O_4$, 2)$Ce_{0.05}P_{0.05}Mg_{0.9}Al_2O_4$ and 3)$Ce_{0.1}P_{0.1}Mg_{0.8}Al_2O_4$ samples at 800, 1000 and 1200°C.

Table 3 Color coordinates for different samples at 800, 1000 and 1200°C

T,°C	Composition	Color parameter					En. gap
		L*	a*	b*	C*	H°	ΔE, eV
800	$MgAl_2O_4$	98.3	-0.16	0.34	0.38	64.8	3.76
	$Ce_{0.05}Pr_{0.05}Mg_{0.9}Al_2O_4$	88.20	2.37	6.35	6.77	69.5	2.1
	$Ce_{0.1}Pr_{0.1}Mg_{0.8}Al_2O_4$	76.59	6.1	9.71	11.5	57.86	1.88
1000	$MgAl_2O_4$	97.97	-0.16	0.45	0.48	70.43	3.26
	$Ce_{0.05}Pr_{0.05}Mg_{0.9}Al_2O_4$	75.77	5.1	11.1	12.22	65.3	1.94
	$Ce_{0.1}Pr_{0.1}Mg_{0.8}Al_2O_4$	69.45	7.92	9.5	12.37	50.25	1.75
1200	$MgAl_2O_4$	97.9	0.07	0.78	0.78	84.9	2.95
	$Ce_{0.05}Pr_{0.05}Mg_{0.9}Al_2O_4$	70.94	6.1	11.87	13.3	63.2	191
	$Ce_{0.1}Pr_{0.1}Mg_{0.8}Al_2O_4$	63.66	9.49	11.61	15	50.73	1.7

3.6 Uv-Visible spectra

Figure 4 shows the uv-visible absorption spectra for the investigating samples oxides. Cerium oxide has a strong absorption at 450 nm, which is originated in the O_{2p}–Ce_{4f} charge transfer transitions. The doping by Pr^{4+} ions, the band gap reducing from 2.1 to 1.91 eV for $Ce_{0.05}P_{0.05}Mg_{0.9}Al_2O_4$ and from 1.88 to 1.7 eV for $Ce_{0.1}P_{0.1}Mg_{0.8}Al_2O_4$ which shifted to the red absorption edge.

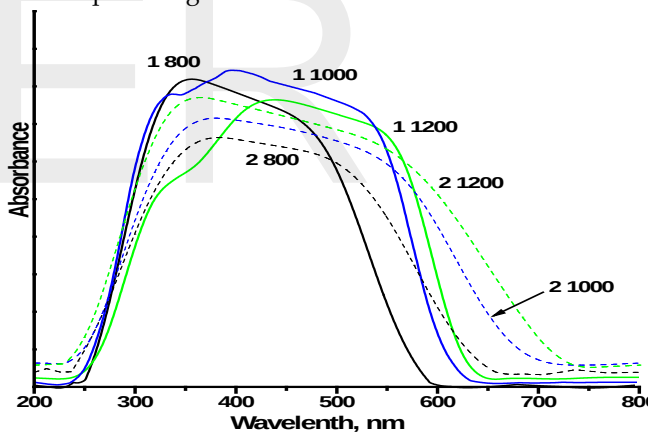

Fig 4. Uv-Visible spectra of 1)$Ce_{0.05}P_{0.05}Mg_{0.9}Al_2O_4$ and 2)$Ce_{0.1}P_{0.1}Mg_{0.8}Al_2O_4$ samples at 800, 1000 and 1200°C.

4 Conclusions

$Ce_xPr_xMg_{1-2x}Al_2O_4$ ceramic pigments were synthesized by combustion method using malonic acid dihydrazide as a fuel following by annealing at 800, 1000 and 1200oC. Pigment powder characterized by different tools as thermal analysis (TG-DTA), x-ray diffractions (XRD), transmission electron microscopy (TEM) and infrared spectroscopy (IR) and diffuse reflectance spectroscopy (DRS) using CIE-L*a*b* parameters method for color measurements. Yellow red pigments were produced from $CePrO_{2-\delta}$ phase as result of charge transfer transition between O_{2p} and Ce_{4f} and reduce the band gap from 2.76 to 1.7 eV.

5 Reference

[1] Cox J. D., Pilcher G., thermochemistry of organic and organometallic compounds, Academic Press, New York, pp.1-636, 1970.

International Journal of Scientific & Engineering Research, Volume 4, Issue 8, August 2013
ISSN 2229-5518

[2] Kibler G.M., Hunt H., Heats of combustion.V. The heats of combustion of five nitrogen-containing compounds, J. Phys. Chem., v.53, pp. 955-956, 1949.
[3] Patil K.C., Hegde M.S., Rattan T., Aruna S.T., chemistry of combustion synthesis, properties and applications: nanocrystalline oxide materials, World Scientific Publishing Co. Pte. Ltd., London, 2008, pp. 1-362.
[4] A. Saberi, F. Golestani-Fard, H. Sarpoolaky, M. Willert-Porada, T. Gerdes and R. Simon, chemical synthesis of nanocrystalline magnesium aluminate spinel via nitrate–citrate combustion route, J. Alloys Compds, 462, 142–146, 2008.
[5] Kakooei S., Rouhi J., Mohammadpour E., Alimanesh M. and Dehzangi, A. synthesis and characterization of Cr-Doped Al_2O_3 nanoparticles prepared via aqueous combustion method, Caspian Journal of Applied Sciences Research, 1(13),16-22, 2012.
[6] Ganesh I., Reddy G. J., Sundararajan G., Olhero S. M., Torres P. M. C. and Ferreira J. M. F., Influence of processing route on microstructure and mechanical properties of $MgAl_2O_4$ spinel, Ceram. Int., 36, 473–482, 2010.
[7] Chandradass J., Balasubramanian M., Bae D. S., Kim J. and Kim K. H., effect of water to surfactant ratio ® on the particle size of $MgAl_2O_4$ nanoparticle prepared via reverse micelle process, J. Alloys Compds, 491, L25–L28, 2010.
[8] Zawrah M.F., Hamaad H. and Meky S., Synthesis and characterization of nano $MgAl_2O_4$ spinel by the co-precipitated method, Ceram. Int., 33, 969–978, 2007.
[9] Zhang X., hydrothermal synthesis and catalytic performance of high-surface-area mesoporous nanocrystallite $MgAl_2O_4$ as catalyst support, Mater. Chem. Phys., 116, 415–420, 2009.
[10] Saberi A., Golestani-Fard F., Willert-Porada M., Negahdari Z., Liebscher C. and Gossler B., a novel approach to synthesis of nanosize $MgAl_2O_4$ spinel powder through sol–gel citrate technique and subsequent heat treatment, Ceram. Int., 35, 933–937, 2009.
[11] Zhang H., Jia X., Liu Z. and Li Z., The low temperature preparation of nanocrystalline $MgAl_2O_4$ spinel by citrate sol–gel process, Mater. Lett., 58, 1625– 1628, 2004.
[12] Aruna S. T. and Mukasyan A. S., combustion synthesis and nanomaterials, Curr. Opin. Solid State Mater. Sci., 12, 44–50, 2008.
[13] Prabhakaran K., Patil D.S., Dayal R., Gokhale N.M. and Sharma S.C., Synthesis of nanocrystalline magnesium aluminate (MgAl2O4) spinel powder by the urea–formaldehyde polymer gel combustion route, Mater. Res. Bull., 44, 613–618, 2009.
[14] Bai J., Liu J., Li C., Li G. and Du Q., mixture of fuels approach for solution combustion synthesis of nanoscale $MgAl_2O_4$ powders, Adv. Powder Technol., 22, 72–76, 2011.
[15] Alinejad B., Sarpoolaky H., Beitollahi A., Saberi A. and Afshar S., synthesis and characterization of nanocrystalline $MgAl_2O_4$ spinel via sucrose process, Mater. Res. Bull., 43, 1188–1194, 2008.
[16] Ianos R., Lazau I., Pacurariu C. and Barvinschi P., Solution combustion synthesis of $MgAl_2O_4$ using fuel mixtures, Mater. Res. Bull., 43, 3408–3415, 2008.
[17] Alvar E. N., Rezaei M. and Alvar H. N., Synthesis of mesoporous nanocrystalline $MgAl_2O_4$ spinel via surfactant assisted precipitation route, Powder Technol., 198, 275–278, 2010.
[18] Li F., Zhaoa Y., Liua Y., Haoa Y., Liua R., Zhaob D., solution combustion synthesis and visible light-induced photocatalytic activity of mixed amorphous and crystalline $MgAl_2O_4$ nanopowders. Chem. Eng. J., 173, 750– 759, 2011.
[19] Jiang S., Lua T., Zhanga J., Chen J., first-principles study on the effects of point vacancies on the spectral properties of $MgAl_2O_4$, Solid State Commun., 151, 29–32, 2011.